Ligand binding and heterodimerization with retinoid X receptor α (RXRα) induce farnesoid X receptor (FXR) conformational changes affecting co-activator binding

Na Wang[1, 2, 3], Qingan Zou[4], Jinxin Xu[2, 3], Jiancun Zhang[2, 3, 4], Jinsong Liu[2, 3*]

[1] School of Life Sciences, University of Science and Technology of China, Hefei, 230026, China

[2] State Key Laboratory of Respiratory Disease, Guangzhou Institutes of Biomedicine and Health, Chinese Academy of Sciences, Guangzhou, 510530, China

[3] Guangdong Provincial Key Laboratory of Biocomputing, Guangzhou Institutes of Biomedicine and Health, Chinese Academy of Sciences, Guangzhou, 510530, China

[4] Guangzhou Henovcom Biosciences Inc, Guangzhou, 510530, China

Running title: Allosteric signal transduction in FXR/RXR heterodimer

*To whom correspondence should be addressed: Jinsong Liu, Telephone: +86 20 32015317, Fax: +86 20 32015299, E-mail address: liu_jinsong@gibh.ac.cn

Keywords: Farnesoid X receptor (FXR), Retinoid X receptor (RXR), transcription factor, signal transduction, X-ray crystallography, metabolism, allostery, conformational change

Table S1. Peptide binding by fluorescence anisotropy

Receptors	FXR/RXR ligands	Dissociation constants (μM)
FXR-LBD	apo	6.60±0.33
FXR-LBD/RXR-LBD•SRC1	apo/apo	2.42±0.27
	HNC143	0.71±0.07
	HNC143/9cRA	0.58±0.06
	HNC180	0.51±0.04
	HNC180/9cRA	0.46±0.05
	GW4064	0.73±0.07
	GW4064/9cRA	0.43±0.05
RXR-LBD	apo	4.30±0.64
FXR-LBD•SRC1/RXR-LBD	apo/apo	2.12±0.08
	9cRA	0.70±0.01
	HNC143/9cRA	0.48±0.24
	HNC180/9cRA	0.31±0.16
	GW4064/9cRA	0.50±0.10

Table S2. Interactions in the RXRα/FXR dimer interface

Non-polar interactions			Polar interactions		
RXRα		FXR	RXRα		FXR
(H9)	Y397-A431	(H11)	(H7)	D379-R436	(H11)
(H9)	Y397-R436	(H11)	(H7)	K356-E405	(H9)
(H9)	A398-Q428	(L9)	(H11)	R426-T442	(H11)
(H11)	F415-A431	(H11)	(H11)	S427-R441	(H11)
(H11)	A416-F430	(H11)	(H11)	K417-E405	(H9)
(H11)	L419-L434	(H11)	(H11)	K417-E409	(H9)
(H11)	L420-L434	(H11)	(H11)	R421-D394	(L8)
(H11)	L420-L412	(H9)	(H11)	R426-E439	(H11)
(H11)	L420-L437	(H11)	(H11)	E434-H445	(H11)
(H11)	P423-T438	(H11)			
(H11)	L430-T442	(H11)			

Residues involved in dimerization are listed along with the secondary structures. The intermolecular interactions are grouped into polar and nonpolar interactions. The nonpolar interactions include Vander Waals contacts and hydrophobic interactions with a distance cutoff 4.5 Å, and the polar interactions include charged interactions (4 Å cutoff) and hydrogen bonds (3.5 Å cutoff)

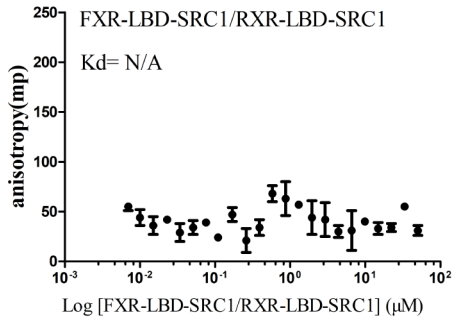

Supporting Fig. 1. Characterization of the interaction between coactivator and FXR-LBD•SRC1/RXR-LBD•SRC1. No interaction was observed between the fluorescein-labeled peptide and FXR-LBD•SRC1/RXR-LBD•SRC1.

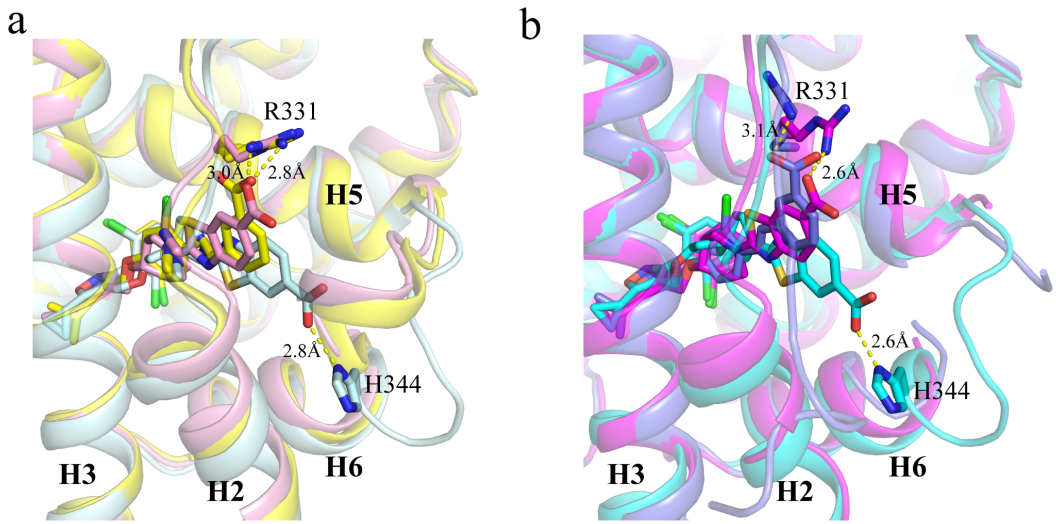

Supporting Fig. 2. Conformation induced by ligands in FXR-LBD and FXR/RXR-LBD structure. (a) Alignment of FXR-LBD structures with three different ligands show the conformation difference between helix 5 and helix 6. (HNC143-FXR-LBD, pale cyan; HNC180-FXR-LBD, pink; GW4064-FXR-LBD, yellow). (b) Alignment of three FXR/RXR-LBD structures. (HNC143-FXR/9cRA-RXR, cyan; HNC180-FXR/9cRA-RXR, magenta; GW4064-FXR/9cRA-RXR, slate). Hydrogen bond is labeled as dashed line, colored yellow.

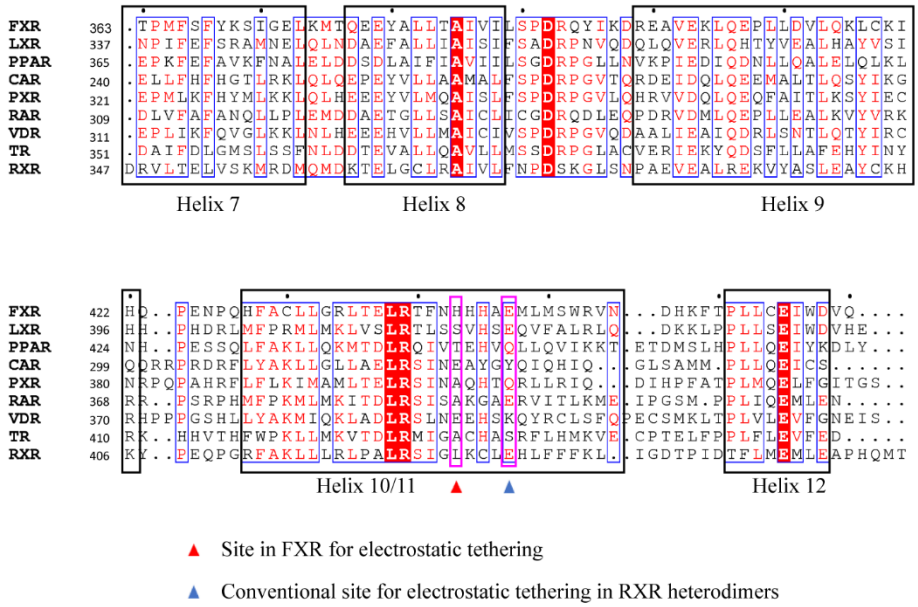

Supporting Fig. 3. Structure-based sequence alignment of RXR nuclear receptor partners

Only the regions that are involved in the dimerization interface are shown. The secondary structures are noted under the sequences.

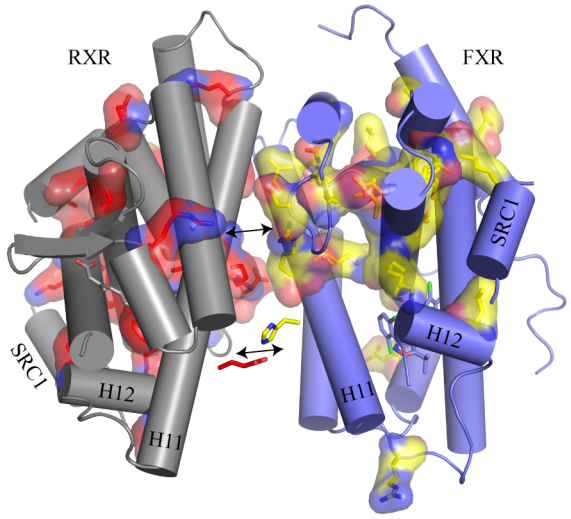

Supporting Fig. 4. Schematic diagram summarizing the signal pathway through the heterodimer interface. The SCA network residues are plotted on FXR and RXR using the GW4064-FXR/9cRA-RXR crystal structure as a model. Residues participated in electrostatic tethering are shown as sticks. Arrows indicate the signal transduction pathway through the heterodimer interface.

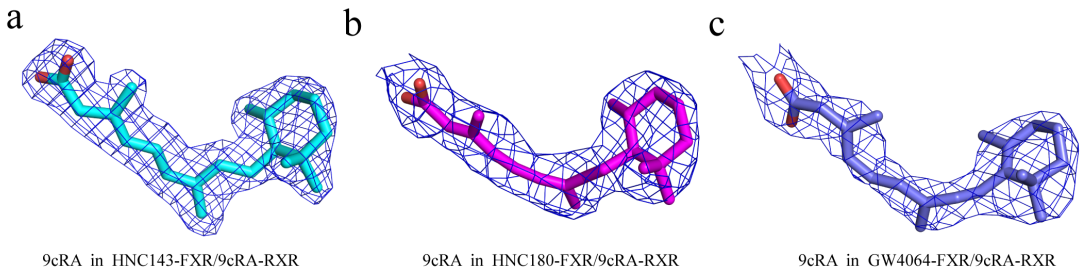

Supporting Fig. 5. Electron density maps for 9cRA in the three FXR/RXR heterodimers. (a-c) Electron density maps for 9cRA within the RXR pockets in the three heterodimers as labeled in the figure. The maps were calculated with σ_A-weighted 2Fo-Fc coefficients and contoured at 1.0σ.

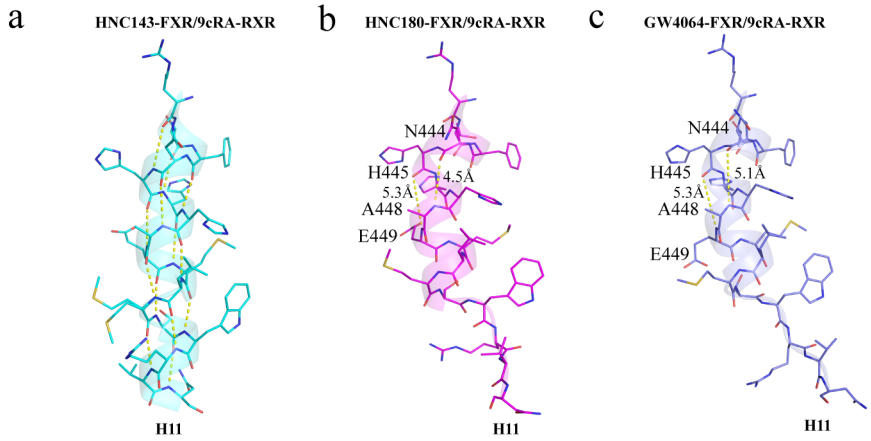

Supporting Fig. 6. Secondary structure changes in the C terminus of H11 in FXR in three ligands bound heterodimers. (a) In HNC143 bound heterodimer, the C terminus of H11 has a normal hydrogen bond network, while main chain hydrogen bonds formed by N444-E448, H445-E449 are lost in (b) HNC180 and (c) GW4064 bound heterodimers.

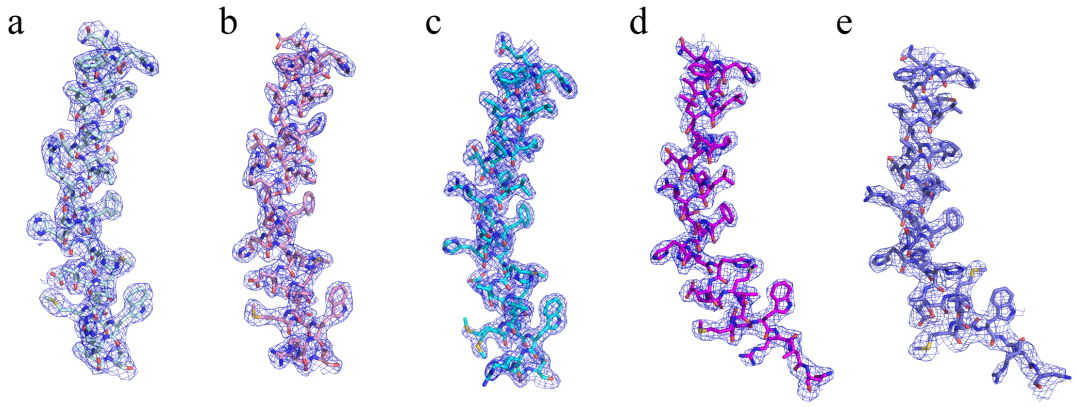

Supporting Fig. 7. Electron density maps for FXR Helix 11 in two FXR monomers and three FXR/RXR heterodimers. (a-e) Electron density maps for FXR Helix11 (a) in HNC143-FXR (pale cyan), (b) HNC180-RXR (pink), (c) HNC143-FXR/9cRA-RXR (cyan), (d) HNC180-FXR/9cRA-RXR (magenta), (e) GW4064-FXR/9cRA-RXR (slate). The maps were calculated with 2Fo-Fc coefficients and contoured at 1.0σ.

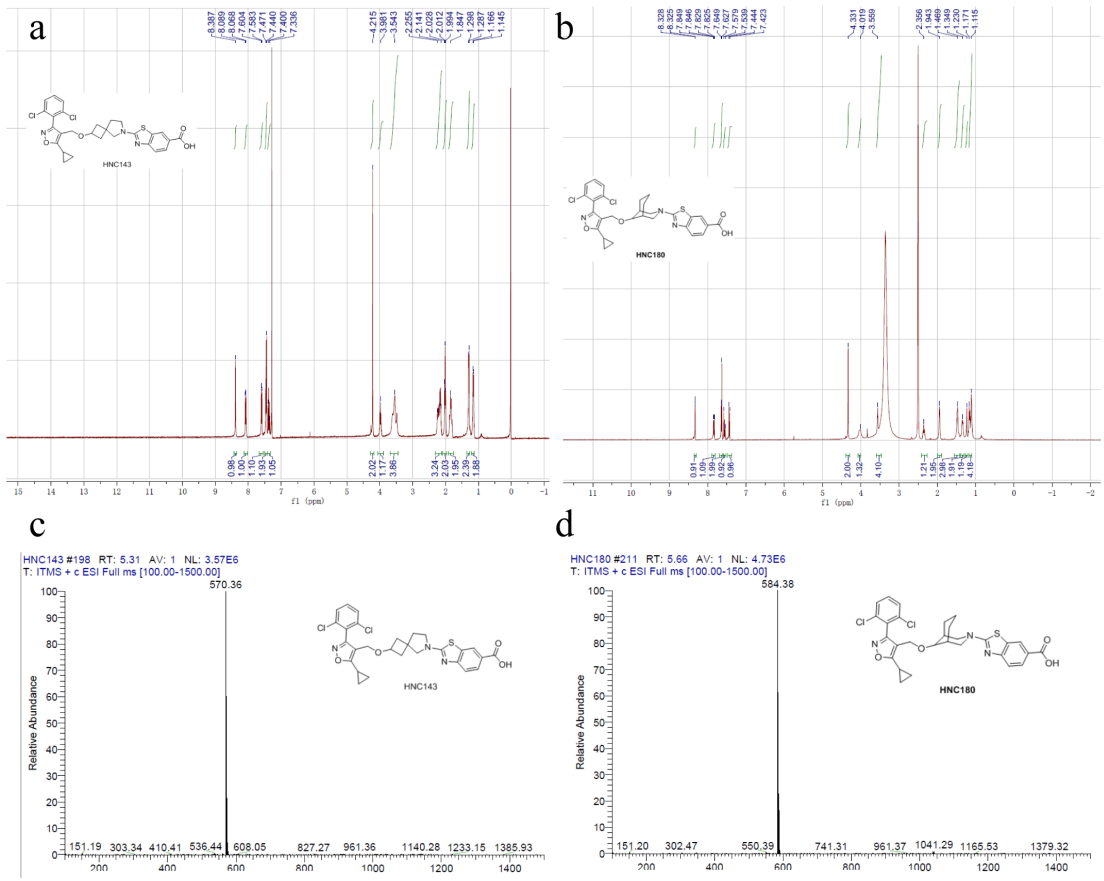

Supporting Fig. 8. ^{1}H-NMR spectra and Mass Spectra data. (a-b) ^{1}H-NMR spectra of HNC143 and HNC180. (c-d) Mass Spectra data of HNC143 and HNC180.